



# Photophysical and optical properties of 5-Bromo-2-nitropyridine organic molecule: Experiment and theory

Bayram Gündüz<sup>a</sup>, Mustafa Kurban<sup>b,\*</sup>

<sup>a</sup> Department of Science Education, Faculty of Education, Muş Alparslan University, 49250, Muş, Turkey

<sup>b</sup> Department of Electronics and Automation, Ahi Evran University, 40100, Kırşehir, Turkey

## ARTICLE INFO

### Keywords:

Organic molecules  
Photophysical properties  
Electronic structure  
Density-functional theory  
Refractive index

## ABSTRACT

The changes in the structural, electronic, vibrational and optical properties of 5-Bromo-2-nitropyridine organic molecule have been investigated. The semi-empirical realtions have been proposed for the calculation of the refractive index ( $n$ ). The energy gap ( $E_g$ ), harmonic frequencies, Mulliken atomic charges, density of states (DOS), radial distribution functions (RDFs) and coordination number of binary interactions were searched. Ultraviolet–visible (UV–Vis) spectral analysis has been carried out using experimental techniques and time-dependent (TD) DFT calculations. The stability of the organic compound changes based on solvent environment.  $E_g$  decreases depending on increase in the concentration. The compound in chloroform is more stable than that of the other solvents. The theoretical calculations are consistent with the experimental results.

## 1. Introduction

Organic semiconductors have attracted great attention as potential advanced materials used in many electronic, optoelectronic, and photonic applications [1] such as solar cells [2–5] photovoltaics [4,5] light emitting diodes [4,6] sensors [7,8], chemical sensors [9], vapour sensors [10], gas sensors [11,12] and photodetectors [13]. Among the semiconductors, small molecule semiconductor materials in combination with polymer binders and suitable solvents are the most widely used in areas including the field of organic electronic applications [14,15] because they potentially provide high-quality chain alignment and can be reliably synthesized with accurate molecular weight control without significant batch-to-batch variations, [16,17].

To date there have been no studies about the structural, electronic, spectroscopic and optical properties of the 5-Bromo-2-nitropyridine small organic molecule. Fourier Transform Infrared (FT-IR) and Fourier Transform Raman (FT-Raman) spectra characteristics were investigated using quantum chemical calculations [18]. In this study, the structural, electronic vibrational, optical properties of the related material were investigated in detail for different concentrations and solvents. In this regard, we have analysed the optimized bond distances, angles, vibrational harmonic frequencies, process of geometry optimization, refractive index ( $n$ ), radial distribution functions (RDFs) and probability distributions in terms of coordination number of the binary interactions, the highest occupied

molecular orbital (HOMO), the lowest unoccupied molecular orbital (LUMO), the frontier molecular orbital energy gap (HOMO–LUMO difference in energy gap,  $E_g$ ), Mulliken atomic charges (MAC) and density of state (DOS) of the small molecule using density functional theory (DFT) calculations. Using time-dependent (TD)-DFT method, the theoretically predicted the ultraviolet–visible (UV–Vis), HOMO, LUMO and  $E_g$  of the small molecule have been compared with the measured results and discussed in detail.

## 2. Experimental details

Solution technique has been used for 5-Bromo-2-nitropyridine small organic semiconductor dye to investigate spectroscopic, electronic and optical properties. The 5-Bromo-2-nitropyridine is provided from Sigma-Aldrich Chemical Company (USA) with a stated purity of 99% (HPLC). The solutions of the 5-Bromo-2-nitropyridine have been prepared for 1.304, 1.775 and 3.670  $\mu\text{M}$  and then the weighed 5-Bromo-2-nitropyridine materials were dissolved homogeneously in 13 mL volume of the dichloromethane (DCM) solvent.

## 3. Computational details

The structural, electronic and spectroscopic properties of the small organic material have been investigated using DFT [19] at the B3LYP level [20–22]. The 6-311G (d, p) basis set has been used in the

\* Corresponding author.

E-mail addresses: [mkurbanphys@gmail.com](mailto:mkurbanphys@gmail.com), [mkurban@ahievran.edu.tr](mailto:mkurban@ahievran.edu.tr) (M. Kurban).

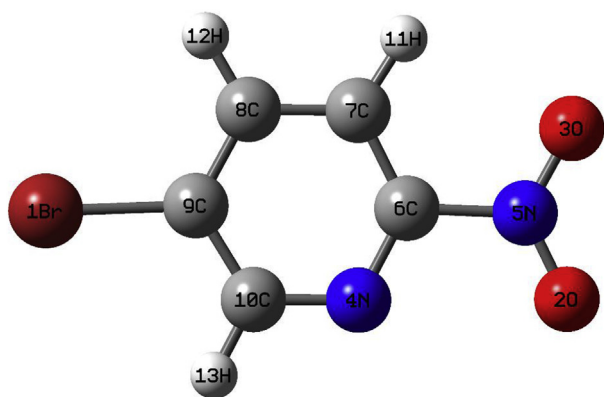


Fig. 1. (Colour online) Optimized ground state geometry of 5-Bromo-2-nitropyridine small organic molecule with atom numbering calculated by B3LYP/6-311-G (d, p). (For interpretation of the references to colour in this figure legend, the reader is referred to the Web version of this article.)

calculations. The calculations have been performed using the GAUSSIAN09 program package [23]. Various spin multiplicities were investigated and it has been found that 5-Bromo-2-nitropyridine have spin singlet as the most stable (minimum total energy). The geometry of 5-Bromo-2-nitropyridine were optimized without imposing any symmetrical constraints and the lowest total energy configuration was assumed as the global minimum case. The structure is taken as the local minima on potential energy surface having positive vibration frequencies. After geometric optimization, TD-DFT method used to get

maximum wavelengths and compared with the experimental UV absorption and  $E_g$  of the 5-Bromo-2-nitropyridine material.

## 4. Results and discussion

### 4.1. Structural analysis

Optimized ground state structure and process of geometry optimization of the 5-Bromo-2-nitropyridine with atom numbering calculated by B3LYP/6-311-G (d, p) is shown in Figs. 1 and 2, respectively. From DFT calculations, the positive vibrational spectra, that is no any kind of imaginary frequency, were found that the optimized geometry is located at stationary point on the potential energy surface. The lowest vibrational harmonic frequencies were found to be 36.16, 37.11 and 38.65 for chloroform, chlorobenzene and DCM, respectively. From these results, one can conclude that the compound in chloroform is more stable than that of the other solvents. The geometrical optimization results reveal that the structure with minimum total energy is the  $C_1$  form. All the 33 fundamental modes of vibrations were found to be IR and Raman active suggesting that the molecule possesses a non-centro symmetric structure. For visual comparison the simulated FT-IR and FT-Raman spectra are shown in Figs. 3 and 4, respectively.

### 4.2. Ultraviolet-visible spectroscopy

The molar extinction coefficient ( $\epsilon$ ), which is also known as the molar absorptivity and molar attenuation coefficient is an intrinsic property of the species. The  $\epsilon$  can be given depends on the Beer-Lamber law [24],

$$\epsilon = \frac{Abs}{CL} \quad (1)$$

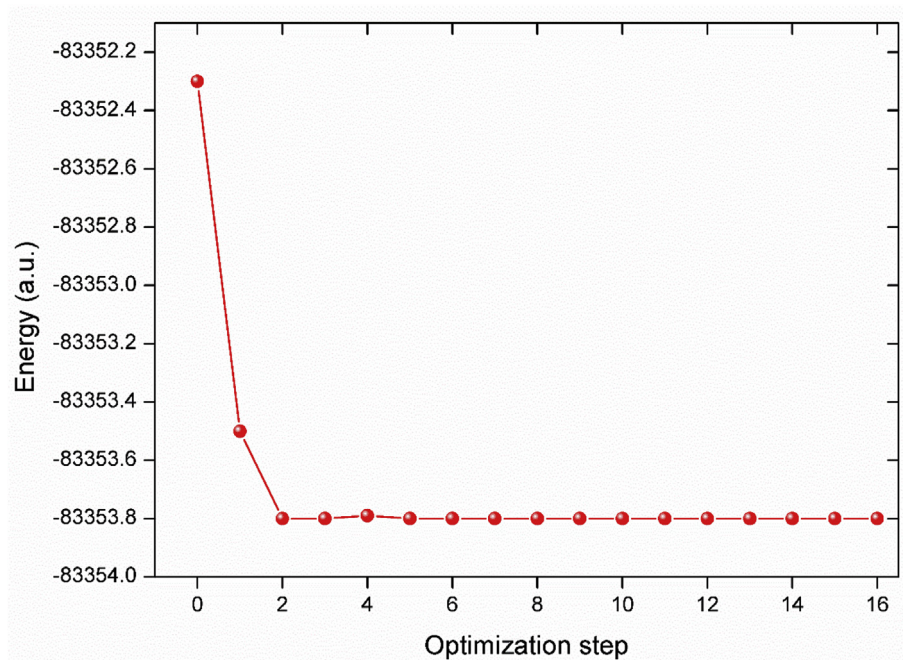


Fig. 2. (Colour online) Process of geometry optimization of the 5-Bromo-2-nitropyridine depending on energy. (For interpretation of the references to colour in this figure legend, the reader is referred to the Web version of this article.)

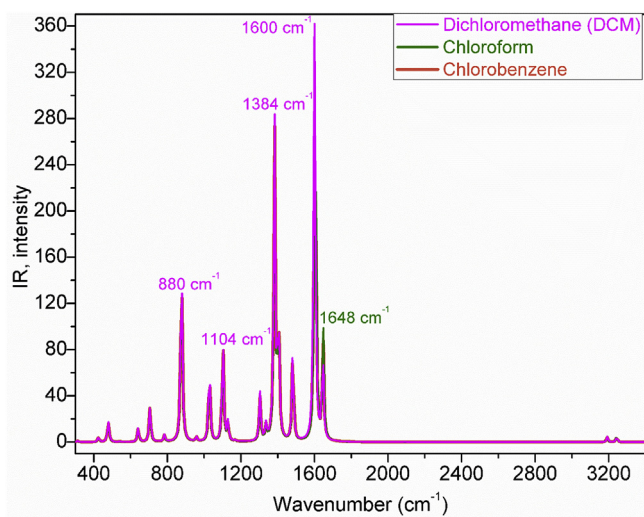


Fig. 3. (Colour online) FT-IR spectra of the 5-Bromo-2-nitropyridine. (For interpretation of the references to colour in this figure legend, the reader is referred to the Web version of this article.)

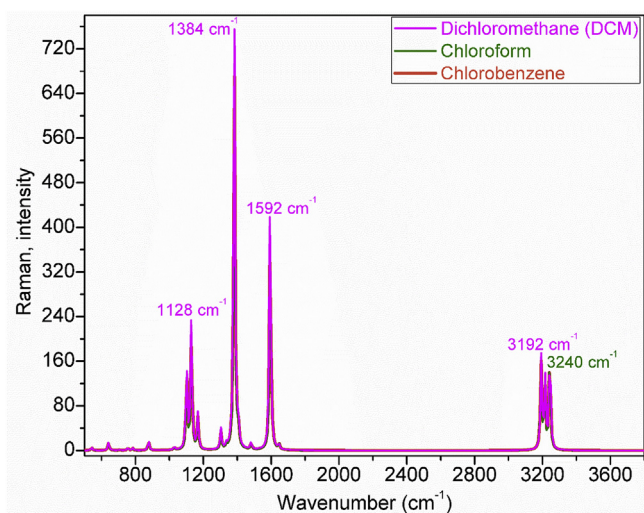


Fig. 4. (Colour online) FT-Raman spectra of the 5-Bromo-2-nitropyridine. (For interpretation of the references to colour in this figure legend, the reader is referred to the Web version of this article.)

where Abs is the absorbance,  $C$  is the concentration of a solution sample and  $L$  is the path length of the sample. The molar absorptivity value of the 5-Bromo-2-nitropyridine for chloroform solvents was experimentally obtained from Eq. (1). Fig. 5(a) indicates the molar absorptivity plots vs. wavelength ( $\lambda$ ) for DCM solvent. As seen in Fig. 5(a), for DCM solvent the experimental and theoretical molar extinction coefficient exhibits maximum values at 282 and 292 nm, respectively. In addition, the experimental and theoretical molar extinction coefficients exhibit one dominant peak in invisible region. Obtained results suggest that the experimental molar extinction coefficient values are compatible with

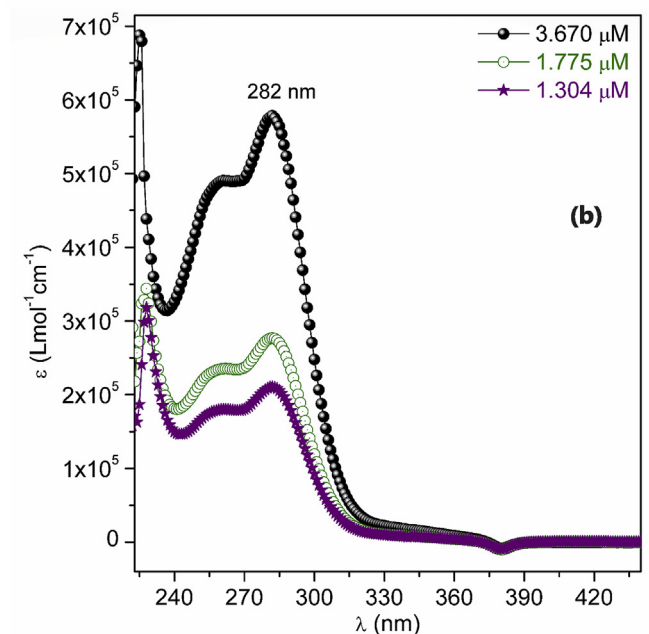
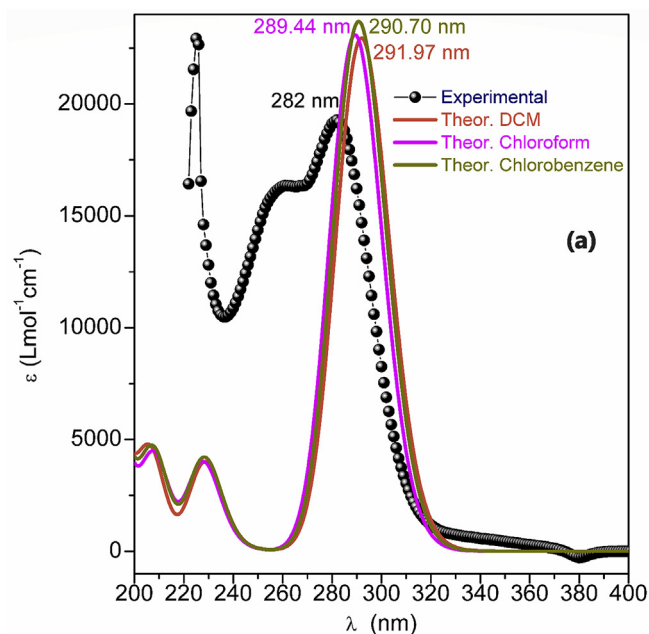


Fig. 5. (Colour online) The molar absorptivity plots vs. wavelength ( $\lambda$ ) of the 5-Bromo-2-nitropyridine for (a) different solvents (experimental and theoretical) and (b) different concentrations. (For interpretation of the references to colour in this figure legend, the reader is referred to the Web version of this article.)

theoretical ones. The theoretical molar extinction coefficients are close to each other as seen in Fig. 5(a). Fig. 5(b) shows the absorbance curves of the 5-Bromo-2-nitropyridine solutions for different concentrations. The absorbance of 5-Bromo-2-nitropyridine decreases with decreasing concentrations. The maximum peak position or wavelength values for 1.304, 1.775 and 3.670  $\mu\text{M}$  were found to be 282 nm. The position of



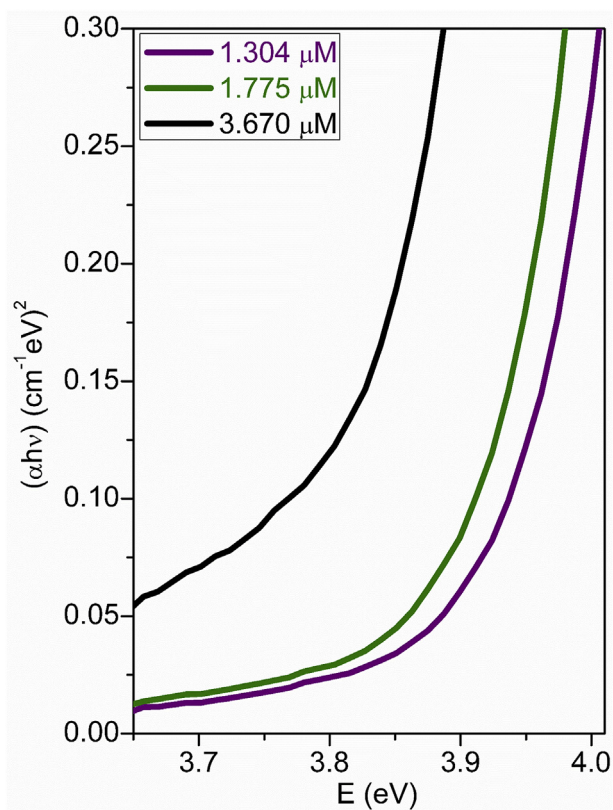


Fig. 6. (Colour online) The  $(\alpha h\nu)^2$  vs photon energy of the 5-Bromo-2-nitropyridine solutions for different concentrations. (For interpretation of the references to colour in this figure legend, the reader is referred to the Web version of this article.)

peaks and corresponding values are displayed in Fig. 5(b). These results indicate that the concentration has significant effect on optoelectronic properties for 5-Bromo-2-nitropyridine solution.

#### 4.3. Electronic band structure

The energy gap which is HOMO–LUMO difference in energy, is an significant parameter in measuring the electron conductivity. Thus, HOMO and LUMO energies were obtained DFT and TD-DFT/B3LYP/6–331 G (d, p) level. The calculated energy value of HOMO is  $-7.731$ ,  $-7.719$ , and  $-7.698$  eV for DFT and  $-7.725$ ,  $-7.414$  and  $-7.692$  eV for TD-DFT in chloroform, chlorobenzene and DCM solvents, respectively. Similarly, LUMO is  $-2.985$ ,  $-2.988$  and  $-2.996$  eV for DFT and  $-2.963$ ,  $-2.965$  and  $-2.970$  eV for TD-DFT in chloroform,

Table 1

The experimental direct optical band gaps ( $E_{gd}$ , eV) and the absorption band edges ( $E_{g-Abs}$ , eV) depending on different solvents and concentrations ( $\mu\text{M}$ ) and the energy gaps ( $E_g$ , eV), obtained from DFT and TD-DFT calculations.

Solvents	DFT	TD-DFT	Conc.	$E_{gd}$	$E_{g-Abs}$
Chloroform	4.730	4.762	1.304	3.881	3.815
Chlorobenzene	4.746	4.748	1.775	3.858	3.781
Dichloromethane	4.701	4.722	3.670	3.747	3.691

chlorobenzene and DCM solvents, respectively. From HOMO–LUMO difference, we have obtained the  $E_g$  values from quantum chemical calculations.

In addition, the measured results exhibit that from the linear region [25] (the best fitting of results) of the variation of  $(\alpha h\nu)^2$  versus E (see Fig. 6), the type of electron transition is direct allowed transition. The energy gap,  $E_g$  is determined by means of extrapolating the linear region of Fig. 6. The experimental direct optical band gaps  $E_{gd}$  depending on solvent and different concentrations obtained from DFT and TD-DFT calculations are tabulated in Table 1.

As it is seen in Table 1, the energy gap for DCM solvents gives reasonable value. For example, the measured  $E_{gd}$  for DCM solvent is 3.881 eV, which is consistent with the theoretical  $E_g$  value (4.701 eV) obtained from DFT (see Table 1). From the results, one can conclude that DCM solvent with the lowering of the band gaps can be preferred for optoelectronic applications or devices, which prefer lower band gaps because the electronic transfer is easier. It implies that the HOMO–LUMO energy gap for chloroform solvent allows easy excitation of electrons from HOMO to LUMO.

The dispersion of the electronic bands for thicker the 5-Bromo-2-nitropyridine samples also increases due to interacting layers and thus reduces  $E_g$  as it seen in Table 1. We also see that the band gap energies decrease with increase of the size of the materials (see Table 1). This is the most remarkable feature of materials, especially at nano level [26–28].

#### 4.4. Refractive index values obtained from different solvents, concentrations and relations

To obtain the refractive index ( $n$ ) values of the 5-Bromo-2-nitropyridine solved in different solvents, many equations such as Reddy, Ravindra, Kumar-Singh, Herve-Vandamme and Moss [29] were used together with the direct ( $E_{gd}$ ) values. The  $n$  values for chloroform, chlorobenzene and dichloromethane (DCM) solvents from theoretical and for DCM solvent from experimental were calculated by using the related equations. Fig. 7(a) indicates  $n$  curves vs. solvents obtained from DFT calculations for various relations. As seen in Fig. 7(a), the  $n$  values for chloroform and chlorobenzene are the same while the  $n$  values for DCM is slightly different. Similarly,  $n$  values obtained from Ravindra relation are the lowest, while the  $n$  values obtained from Reddy relation are the highest.

In addition, the direct refractive index ( $n_{gd}$ ) values of the 5-Bromo-2-nitropyridine for 1.304, 1.775 and 3.670  $\mu\text{M}$  were obtained by using the related equations mentioned above. Fig. 7(b) indicates  $n_{gd}$  curves vs. concentrations for various relations. As seen in Fig. 7(b), the  $n_{gd}$  values for 3.670  $\mu\text{M}$  are the highest, while the  $n_{gd}$  values for 1.304  $\mu\text{M}$  are the lowest. On the other hand, the  $n_{gd}$  values obtained from Reddy relation are the highest, while the  $n_{gd}$  values obtained from Ravindra relation are the lowest. Obtained results suggest that the  $n_{gd}$  values increase based on the concentration.

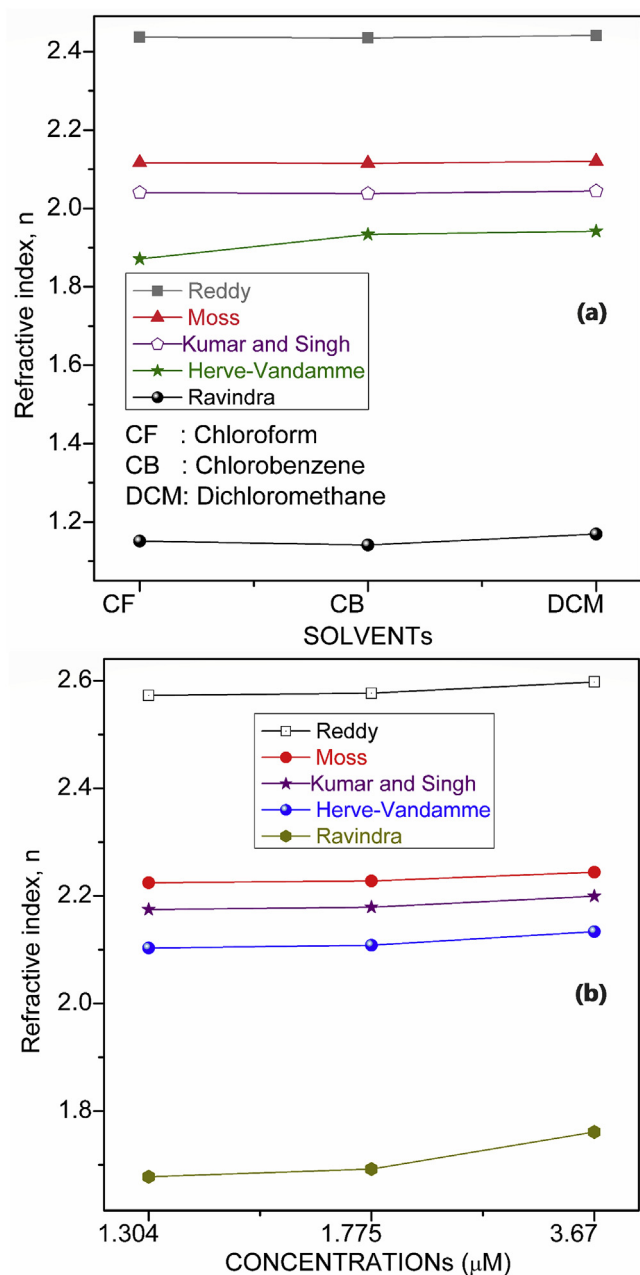


**Fig. 7.** (Colour online) The refractive index ( $n$ ) curves of the 5-Bromo-2-nitropyridine for (a) different solvents (b) 1.304, 1.775 and 3.670  $\mu\text{M}$  obtained from experimental, Reddy, Moss, Kumar-Singh, Hervé-Vandamme and Ravindra relations. (For interpretation of the references to colour in this figure legend, the reader is referred to the Web version of this article.)

#### 4.5. Experimental spectral behaviour of transmittance( $T$ )

The transmittance ( $T$ ) spectra of the solutions of the 5-Bromo-2-nitropyridine for (1.304, 1.775 and 3.670  $\mu\text{M}$ ) are shown in Fig. 8(a).  $T$  spectra of the 5-Bromo-2-nitropyridine organic molecule for

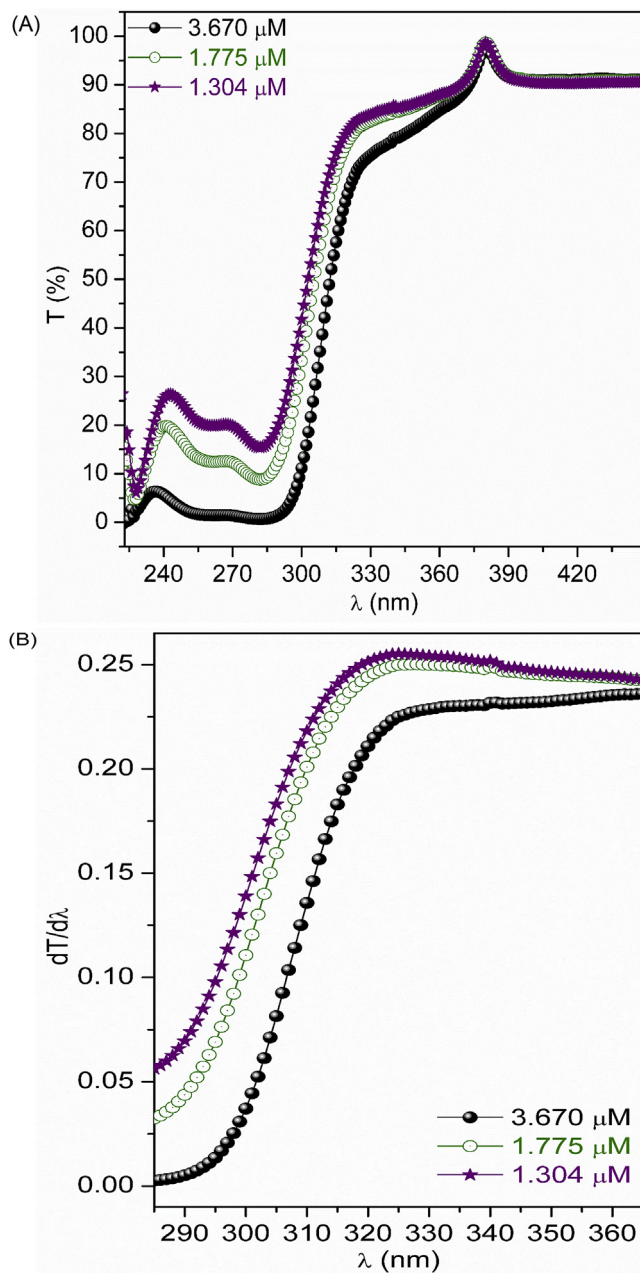


**Fig. 8.** (Colour online) (a) The transmittance ( $T$ ) vs.  $\lambda$  (b)  $dT/d\lambda$  plots vs.  $\lambda$  of the 5-Bromo-2-nitropyridine solutions for different concentrations. (For interpretation of the references to colour in this figure legend, the reader is referred to the Web version of this article.)

different concentrations exhibits minimum trenches at 282 nm. After the minimum tendency of the wavelengths of  $T$ , a sharply increase is observed up to about 390 nm which is maximum constant value of the wavelengths.

The first derivative ( $dT/d\lambda$ ) of  $T$  versus  $\lambda$  are plotted to obtain the

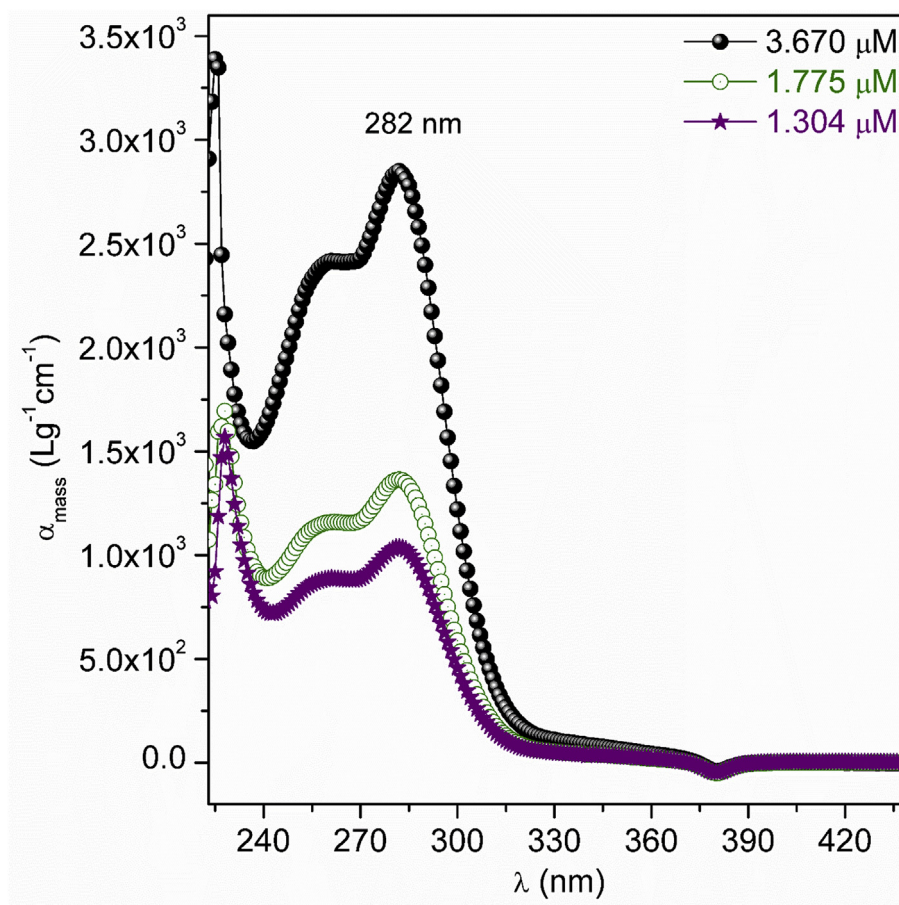


Fig. 9. (Colour online) The mass extinction coefficient ( $\alpha_{mass}$ ) plot vs.  $\lambda$  of 5-Bromo-2-nitropyridine solutions for different concentrations. (For interpretation of the references to colour in this figure legend, the reader is referred to the Web version of this article.)

**Table 2**  
Mulliken atomic charges of 5-Bromo-2-nitropyridine for DCM.

Atoms	Mulliken atomic charges	Atoms	Mulliken atomic charges
Br1	0.028296	C8	0.081347
O2	-0.270784	C9	-0.268769
O3	-0.288679	C10	0.138930
N4	-0.297613	H13	0.155989
N5	0.205688	H13	0.152604
C6	0.326708	H13	0.154873
C7	-0.118589		

absorption band edge ( $E_{g-Abs}$ ) values for different concentrations as seen in Fig. 8(b).  $E_{g-Abs}$  values were obtained using the maximum peak position.  $E_{g-Abs}$  for different concentrations are tabulated in Table 1. As seen in Table 1, the  $E_{g-Abs}$  value decreases with the increase of concentration.

The  $\alpha_{mass}$  values for different concentrations were calculated from Eq. (1). Fig. 9 shows  $\alpha_{mass}$  plot vs. photon energy ( $E$ ) of the 5-Bromo-2-

nitropyridine. As seen in Fig. 9, the mass extinction coefficient varies significantly with photon energy. Obtained results indicate that  $\alpha_{mass}$  values increase with the rise in concentration.

#### 4.6. Theoretical analysis of mulliken atomic charge and dipole moment

The Mulliken atomic charges (MACs) have a significant for quantum



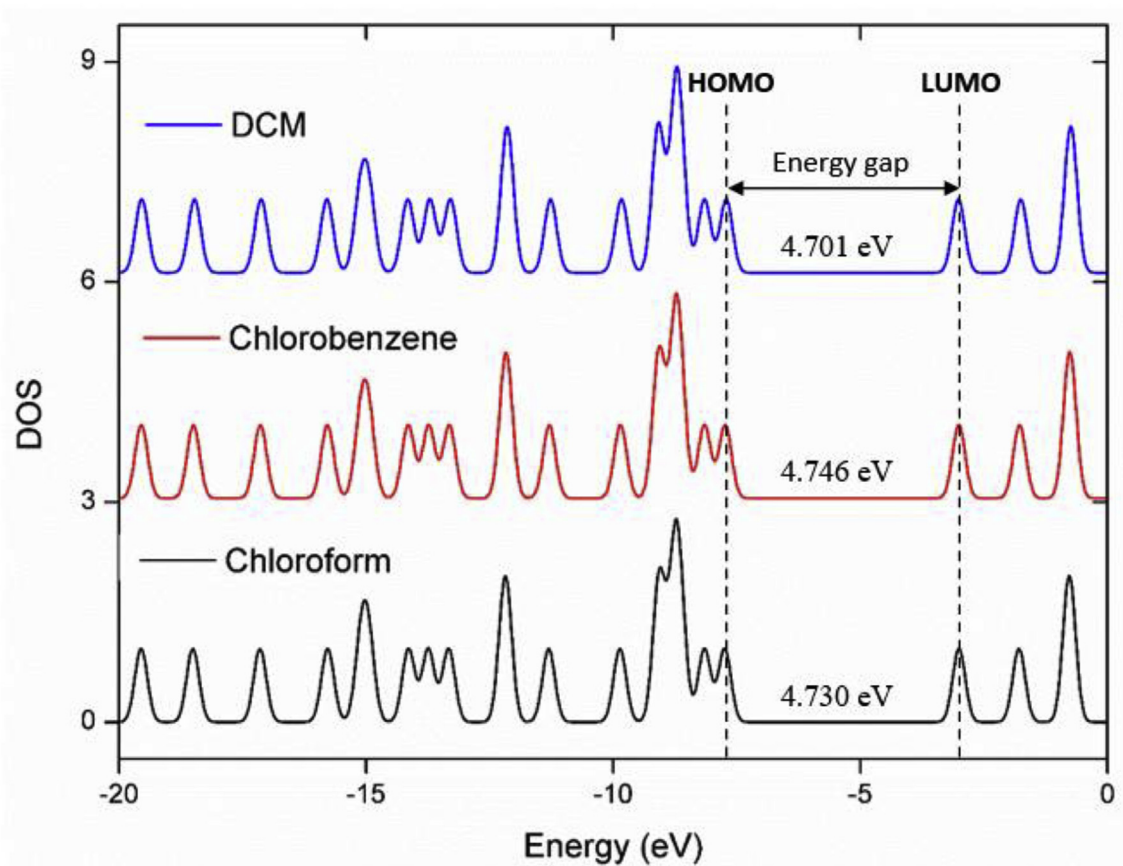


Fig. 10. (Colour online) Density of state (DOS) spectrum of 5-Bromo-2-nitropyridine in DCM, chlorobenzene and chloroform solvents obtained from Mulliken population analysis. (For interpretation of the references to colour in this figure legend, the reader is referred to the Web version of this article.)

mechanical applications. MACs of the 5-Bromo-2-nitropyridine were gathered in Table 2. The charges of the same atoms in the different positions show different charge with each other for the atoms in the 5-Bromo-2-nitropyridine compound. For example, the value of MAC of the C6 atom exhibits a positive charge and it is bigger than others. Hydrogen atom exhibits a positive charge because it is an acceptor atom.

The dipole moments are other important electronic properties. The bigger the dipole moment represents the stronger intermolecular interaction. The highest value of component of dipole moment along the x-axis ( $\mu_x = 6.095$  Debye) predicts large charge separation. The corresponding total dipole moment calculated to be 6.615 Debye. DCM has bigger dipole moment than that of chloroform and chlorobenzene solvents. This is compatible with the energy gap values.

#### 4.7. Analysis of density of state

The density of state (DOS) is important, because the occupied and unoccupied molecular orbitals can be seen on DOS spectrum. DOS gives a representation of molecule orbitals (MOs) compositions and their contributions to chemical bonding. Using Mulliken population analysis,

we plotted DOS spectra (see Fig. 10) for 5-Bromo-2-nitropyridine in DCM, chlorobenzene and chloroform solvents. From Fig. 10, the density of localized states has a sharply increasing tendency in the region of between  $-10$  and  $-15$  eV. The DOS analysis also indicates that the energy gap has the highest value (4.74 eV) in Chlorobenzene, therefore it is less reactive compared with other solvents. 5-Bromo-2-nitropyridine with Chloroform is found to be the highest energy of HOMO value ( $-7.73$  eV).

#### 4.8. Radial distribution function and probability density

Fig. 11 shows the radial distribution functions (RDFs) analysis for the carbon-carbon (C–C), carbon-nitrogen (C–N), carbon-hydrogen (C–H), carbon-oxygen (C–O) and carbon-bromine (C–Br) interactions. of the 5-Bromo-2-nitropyridine. The RDFs was calculated for each atomic pairs. One can see that C–C has a narrower and higher distribution than the other pair interactions because of C–C double bonds which is stronger than one bond. There also is a difference between the interactions. For example, for C atoms, C–O is shorter than C–C, C–N, C–H and C–Br interactions; for all of the combinations, C–C has stronger interactions than the other ones. To study the

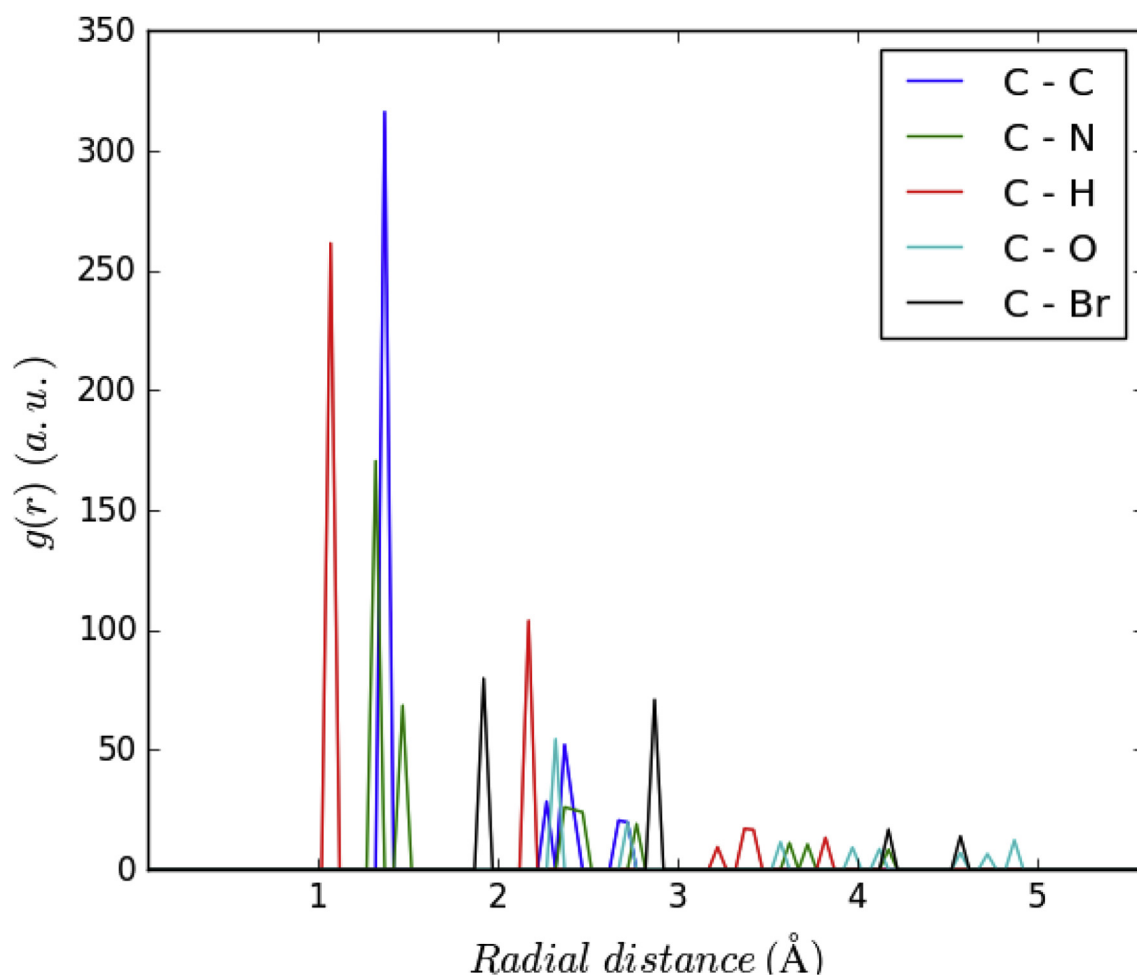


**Fig. 11.** (Colour online) Radial distribution functions (RDFs) of the carbon-carbon (C–C), carbon-nitrogen (C–N), carbon-hydrogen (C–H), carbon-oxygen (C–O) and carbon-bromine (C–Br) interactions. (For interpretation of the references to colour in this figure legend, the reader is referred to the Web version of this article.)

influence of interactions of the atoms in the molecule, we also performed the probability distribution depending on the coordination number (see Fig. 12). The coordination number of C–C, C–Br and C–O interactions significantly decrease while it increases for C–N and C–H interactions.

## 5. Conclusions

5-Bromo-2-nitropyridine small organic molecule have been investigated using experimental and theoretical techniques. The results showed that the structure with minimum total energy is the  $C_1$  form. The maximum peak of experimental molar extinction coefficients for DCM solvent and different concentrations is found to be compatible with theoretical value. The increase in the concentration causes an increase in the direct refractive index values. Bond distances and angles are compatible with available experimental results. From the lowest vibrational frequencies, the compound in chloroform is found to be more

stable than that of the other solvents. The increase in concentration gives rise to the dispersion of the electronic bands thus the band gap energies decrease. Predicted band energy values for different solvents are also agreement with the experimental data. In addition, C–C interactions has a narrower and higher distribution. Optical band gaps and refractive indices of the molecule were controlled with different concentrations and solvent environments.

## Acknowledgments

The numerical calculations reported in this paper were partially performed at TUBITAK ULAKBIM, High Performance and Grid Computing Centre (TRUBA resources). This work was supported by the Ahi Evran University Scientific Research Projects Coordination Unit. Project Number: TBY.E2.17.008, Turkey.



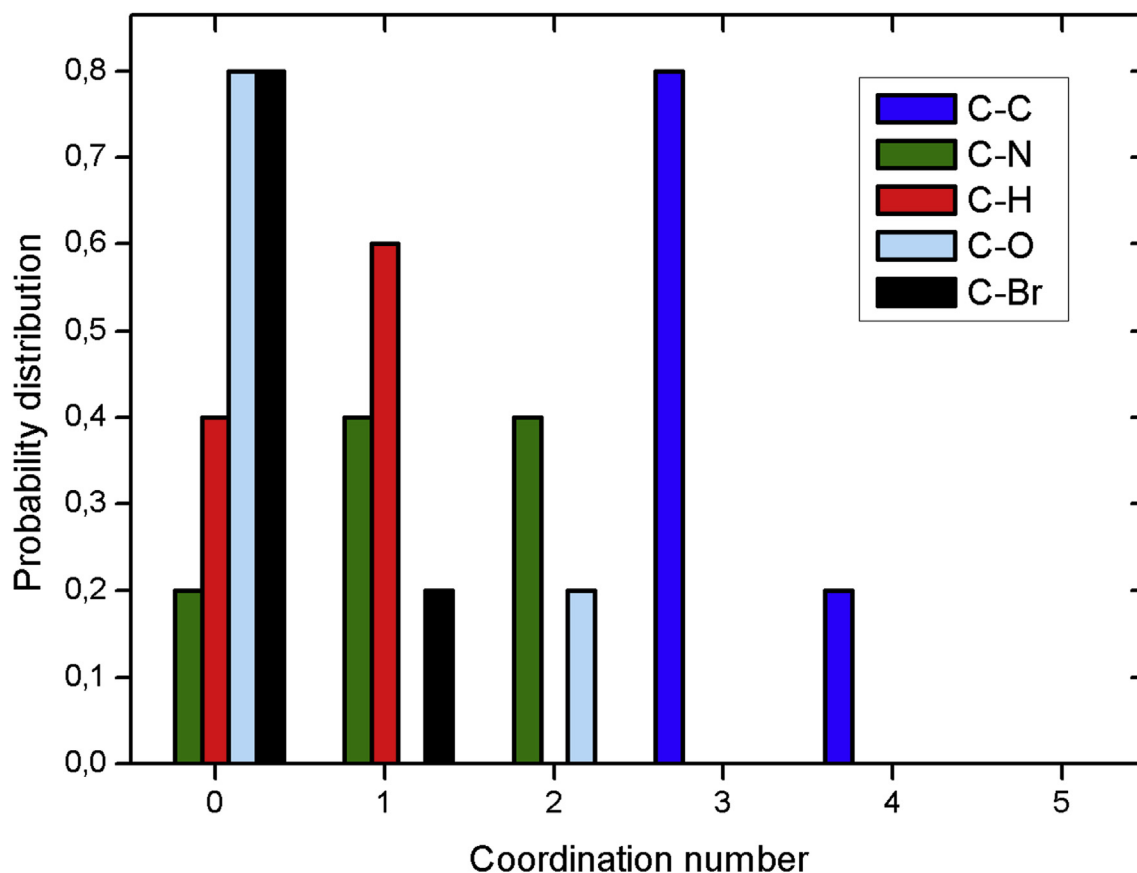


Fig. 12. (Colour online) Probability distributions of the carbon-carbon (C–C), carbon-nitrogen (C–N), carbon-hydrogen (C–H), carbon-oxygen (C–O) and carbon-bromine (C–Br) interactions. (For interpretation of the references to colour in this figure legend, the reader is referred to the Web version of this article.)

## References

- [1] C. Xie, P. You, Z. Liu, L. Li, F. Yan, *Light Sci. Appl.* 6 (2017) e1702.
- [2] T. Hori, T. Masuda, N. Fukuoka, T. Hayashi, Y. Miyake, T. Kamikado, H. Yoshida, A. Fujii, Y. Shimizu, M. Ozaki, *Org. Electron.* 13 (2012) 335.
- [3] A. Migalska-Zalas, I.V. Kityk, M. Bakasse, B. Sahraoui, *Spectrochim. Acta, Part A* 69 (2008) 178.
- [4] A.D. Sio, C. Lienau, *Phys. Chem. Chem. Phys.* 19 (2017) 18813.
- [5] M.Y. Ameen, T. Abhijith, D. Susmita, S.K. Ray, V.S. Reddy, *Org. Electron.* 14 (2013) 554.
- [6] M. Neghabia, A. Behjata, *Curr. Appl. Phys.* 12 (2012) 597.
- [7] F. Aziz, M.H. Sayyad, K. Sulaiman, B.Y. Mailis, K.S. Karimov, Z. Ahmad, G. Sugandi, *Meas. Sci. Technol.* 23 (2012) 014001.
- [8] M. Murugavelu, P.K.M. Imran, K.R. Sankaran, S. Nagarajan, *Mater. Sci. Semicond. Process.* 16 (2013) 461.
- [9] D. Liu, Y. Chu, X. Wu, J. Huang, *Sci. China Math.* 60 (2017) 977.
- [10] R.N. Gillanders, Ifor D.W. Samuel, G.A. Turnbull, *Sensor. Actuator. B Chem.* 245 (2017) 334.
- [11] Y. Huang, R. Yuan, S. Zhou, *J. Mater. Chem.* 22 (2012) 883.
- [12] Y. Huang, L. Fu, W. Zou, F. Zhang, *New J. Chem.* 36 (2012) 1080.
- [13] J.B. Wang, W.L. Li, B. Chu, C.S. Lee, Z.S. Su, G. Zhang, S.H. Wu, F. Yan, *Org. Electron.* 12 (2011) 34.
- [14] A. Migalska-Zalas, *Opt. Quant. Electron.* 48 (2016) 183.
- [15] Y. El Kouari, A. Migalska-Zalas, A.K. Arof, B. Sahraoui, *Opt. Quant. Electron.* 47 (2015) 1091.
- [16] T.K. An, S.-M. Park, S. Nam, J. Hwang, S.-J. Yoo, M.-J. Lee, et al., *Sci. Adv. Mater.* 5 (9) (2013) 1323.
- [17] J. Zhang, G. Wu, C. He, D. Deng, Y. Li, *J. Mater. Chem.* 21 (11) (2011) 3768.
- [18] N. Sundaraganesan, S. Ilakiamani, H. Saleem, Piotr M. Wojciechowski, D. Michalska, *Spectrochim. Acta* 61 (2005) 2995.
- [19] W. Kohn, L.J. Sham, *Phys. Rev.* 140 (1965) A1133.
- [20] A.D. Becke, *Phys. Rev.* 38 (1988) 3098.
- [21] S.H. Vosko, L. Vilk, M. Nusair, *Can. J. Phys.* 58 (1980) 1200.
- [22] C. Lee, W. Yang, R.G. Parr, *Phys. Rev. B* 37 (1988) 785.
- [23] M.J. Frisch, G.W. Trucks, H.B. Schlegel, G.E. Scuseria, M.A. Robb, J.R. Cheeseman, G. Scalmani, V. Barone, B. Mennucci, G.A. Petersson, et al., *Gaussian 09, Revision B.01*, Gaussian, Inc., Wallingford CT, 2009.
- [24] A. Beer, *Ann. Phys.* 86 (1852) 78.
- [25] B. Gündüz, *Opt. Mater.* 36 (2) (2013) 425–436.
- [26] M. Kurban, Ş. Erkoç, *J. Comput. Theor. Nanosci.* 12 (2015) 2605.
- [27] M. Kurban, B. Gündüz, *J. Mol. Struct.* 1137 (2017) 403.
- [28] B. Gündüz, M. Kurban, *Optik* 165 (2018) 370.
- [29] S.K. Tripathy, *Opt. Mater.* 46 (2015) 240.